Technical Physics Letters, 2023, Vol. 49, No. 2

05

Percolative charge transport on electrified surface of polytetrafluoroethylene

© Yu.I. Kuzmin

Ioffe Institute, St. Petersburg, Russia
E-mail: iourk@yandex.ru

Received November 10, 2022
Revised December 8, 2022
Accepted December 9, 2022

The charge transport on the electrically charged surface of polytetrafluoroethylene (PTFE) films in the presence of the adsorption of an electrically conductive phase has been studied. The attenuation of the rate of displacement of the potential drop over the film surface, which limits the area of its expansion, has been found. An estimate has been made for the critical index of the correlation length of a percolation cluster that forms on an electrified PTFE surface at high humidity. It has been experimentally established that the leak of charge from an electrically charged surface is determined by percolation processes.

Keywords: percolation, percolation threshold, adsorption, electrization.

DOI: 10.21883/TPL.2023.02.55368.19422

A model of percolative shunting of an electrified surface (a new type of surface discharge) was proposed in [1]. It differs from common electric discharge [2] in that a part of a surface, which loses the charge accumulated in the process of electrization, is shunted instead of an interelectrode gap. In the present study, the percolative nature of surface discharge of electrified polytetrafluoroethylene (PTFE) films has been established experimentally for the first time. New data on the dynamics of percolative shunting, which allow one both to slow down the discharge process (to ensure stable operation of electrostatic sensors [3–6]) and to speed up the removal of parasitic charges (to protect electronics from electrostatic discharges and enhance the insulation strength [2]), were obtained.

The approach used here relies on the percolation theory [7] to characterize the conductivity of a surface filled partially with a conducting phase that is deposited from the ambient atmosphere (e.g., under the conditions of increased humidity). Owing to its capacity for dissociation into H_3O^+ and OH^- ions, water is a fine conductor of electricity. When a high-conductivity medium interacts with a electrified surface, adsorption stimulated by the electric field is observed. Surface conductivity channels, which shunt the electrified surface, emerge. At small adsorbate concentrations, these channels form isolated clusters. If the degree of surface coverage by a conducting phase increases, a percolation transition occurs: surface conductivity channels merge into an infinite percolation cluster for charge surface to a grounded electrode.

The fraction of the surface area occupied by a conducting adsorbate [1] increases with time:

$$\theta(t) = 1 - \exp\Big(-\int_0^t \alpha(\xi) S\big(R(\xi, t)\big) d\xi\Big), \qquad (1)$$

where $R(\xi, t) \equiv \int_\xi^t v(\eta) d\eta$ is the radius of an adsorbate nucleus, which emerged at point ξ, at time point t; $v = v(t)$ is the nucleus growth rate; $S = S(R)$ is the area of a nucleus with radius R; and $\alpha = \alpha(t)$ is the nucleation rate.

Only the fraction of a surface free from a conducting percolation cluster contributes to surface potential U, since this region is not connected galvanically to a grounded electrode. Thus, $u = 1 - P(\theta)$, where $u \equiv U/U(0)$ is the dimensionless surface potential and P is the density of an infinite cluster. The time dependence of the electrified surface potential is governed by adsorption kinetics (1). Charged particles, which settled onto a surface in the process of electrization, and various structural defects are the primary nucleation centers. Let us use the following law for the nucleation rate: $\alpha(t) = \beta\delta(t)$, where β is the concentration of adsorption centers at the end of electrization and $\delta(t)$ is the Dirac delta function.

At a constant rate of growth of the conducting phase ($v = v_0 = \text{const}$), the entire surface should eventually become conducting and neutralize (see inset *a* in Fig. 1 (curve *1*)). This case is not a typical one: more often than not, the potential decreases at first, reaches a certain limit value U_r, and then remains unchanged for a long period of time. This residual potential section was observed experimentally [8,9] and is used in electret transducers [3,4]. The existence of a discharge characteristic with a residual potential may be attributed to an exponential decay of growth rate $v = v_0 \exp(-t/\tau)$, where τ is the relaxation time [1]. The corresponding potential decay curve is presented in inset *a* of Fig. 1 (curve *2*). One may also notice that the percolation transition (kink of curve $u = u(t')$) at a constant growth rate occurs earlier (curve *1*) than in the

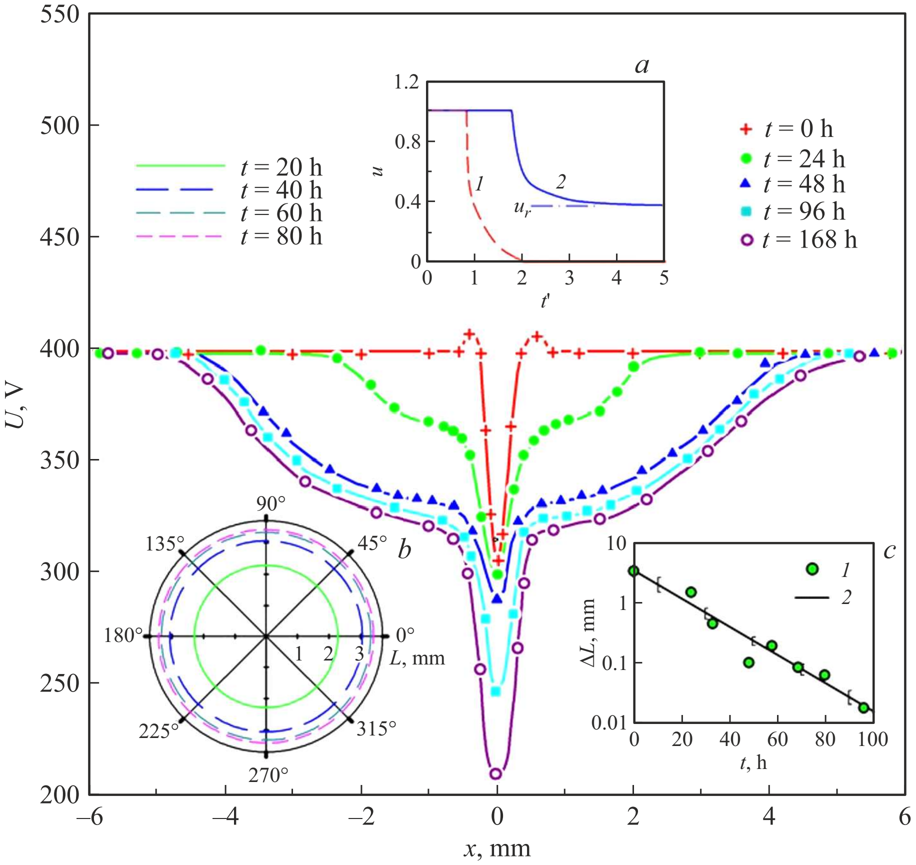

Figure 1. Propagation of a potential drop along an electrified PTFE surface. The charge surface point is at the center of the sample $(x = 0)$. The evolution of the surface potential profile in two opposite directions is presented. Inset *a* shows the potential decay for constant (*1*) and exponentially decaying (*2*) rates of growth of the conducting phase at $\tau' = 1$. The curves in inset *a* are plotted for dimensionless variables: $u \equiv U/U(0)$, $u_r \equiv U_r/U(0)$, $t' \equiv tv_0\sqrt{\pi\beta}$, $\tau' \equiv \tau v_0\sqrt{\pi\beta}$. The kinks of potential decay $u = u(t')$ curves correspond to percolation transitions at $t' = 0.832$ (*1*) and 1.787 (*2*). Inset *b* shows the radial propagation of the potential drop front in 20 h time intervals. Inset *c* presents deviation $\Delta L = L_\infty - L$ of the limit distance traversed by the potential drop front: *1* — experiment, *2* — result of regression analysis at a 5% significance level. The standard error of estimate of regression of the mean ΔL value is indicated.

case of an exponentially decaying rate (curve *2*), since the surface is filled faster with a conducting phase.

To study the dynamics of percolative shunting, we examined F-4 PTFE films with one-sided metallization that were punctured at the center after electrization. Water droplets pulled into the aperture by the edge field established a connection between the electrified surface and grounded metallization; the aperture thus served as a charge surface point. A potential drop emerged as a result at the center of the sample, and the front of this drop propagated along the surface. Samples with a thickness of $10\,\mu$m electrified in a negative corona discharge with a fluid counter electrode (H_2O) to an initial potential of 400 V were stored at 20°C and a relative humidity of 98%. The radial distribution of the surface potential was measured using the compensation method [3] with a vibrating probe $200\,\mu$m in diameter. A DEM-4M electromagnetic transducer excited by a GS-109 signal source served as a vibrator. Compensation of the electric field in the air gap by a constant bias applied to the measurement electrode established open-circuit conditions. The current balance in the external circuit was monitored with a Keithley 6517B electrometer. Measurements were performed in eight directions in steps of 45° in azimuthal angle. Figure 1 shows the propagation of the front of the surface potential drop in two perpendicular directions for one of ten samples. A similar pattern was observed for the other samples: the front propagation slowed down with time, tending to limit value $L_\infty = 3.46$ mm, the spread of which did not exceed 7% within a set of ten samples. This is seen also in inset *b* of Fig. 1, where radial propagation of the front of the potential drop is illustrated. The coordinate of the front was determined at a 50% amplitude with distortions in the charge surface region excluded. With exponential decay of propagation rate $V(t) = V_0 \exp(-t/T)$, the potential drop front traverses over the following distance in time t:

$$L(t) = \int_0^t V(\eta)d\eta = V_0 T\big(1 - \exp(-t/T)\big), \qquad (2)$$

and the limit distance of its travel remains finite: $L_\infty = V_0 T$.

Inset *c* of Fig. 1 presents deviation $\Delta L = L_\infty - L$ of the distance traversed by the potential drop front averaged over eight directions in steps of 45° in azimuthal angle. The results of regression analysis demonstrated that a linear approximation of the time dependence of distance deviation plotted in a semi-logarithmic scale is the optimum one. This confirms the validity of Eq. (2), which implies that $\lg \Delta L \propto t$. The relaxation time, which was determined based on the slope of the curve in inset *c* of Fig. 1, for the propagation rate is $T = 18.62\,\mathrm{h}$. The initial propagation rate of the potential drop front was $V_0 = 5.16 \cdot 10^{-8}\,\mathrm{m/s}$.

According to the concept of universality of critical exponents [10], their values in percolation theory problems depend only on the dimensionality of space. Therefore, the matching between critical indices measured for physical systems, which are proposed to be characterized using the percolation theory, and their known theoretical values proves the validity of the percolation approach. In accordance with the scaling concept [7,11], the correlation length is the only characteristic scale of a percolation cluster in the vicinity of a percolation transition. This means that charge transport along an electrified surface is governed by the conductivity of macroscopic regions with a size on the order of the correlation length, which sets the size of cells of a percolation cluster. When residual potential U_r is reached, percolation length ξ becomes considerably smaller than the sample size (D). Let us assume that relation $\xi \propto D$, which agrees with the scaling concept [11], holds true when the residual potential is reached. Under these conditions, the correlation length is equal, within constant factor λ, to the characteristic sample size: $D = \lambda\xi$. As is known [12], the correlation length of a percolation cluster increases on approach to the percolation threshold, while the cluster density decreases; thus, the surface potential should increase. Therefore, larger samples are expected to have higher limiting residual potential values. In order to verify this assumption, we examined time dependences of the surface potential of electrified samples of different area. These samples were fabricated from an F-4 PTFE film with a thickness of $30\,\mu\mathrm{m}$ and had the shape of squares with side D. Electrization was performed in a negative corona discharge with a fluid counter electrode (H_2O) to a potential of 400 V. The samples were stored on a metal substrate at a humidity of 98% and a temperature of 25°C for three months. The results of measurement of the residual potential are presented in Fig. 2.

Data for $D = 2$, 2.5, 3, 3.5, 4, 4.5 mm were obtained by averaging of the residual potential over ten samples. while data for the remaining points were averaged over five samples. The residual potential varied from 15 to 240 V and increased with sample size. The solid curve in Fig. 2 is the optimum approximation of data derived by regression analysis at a 5% significance level. The potential is, in turn, defined by the percolation cluster density, which depends on the surface coverage by a conducting phase. This provides an opportunity to plot a dependence of the correlation length on the degree of surface coverage by an adsorbate (see Fig. 3).

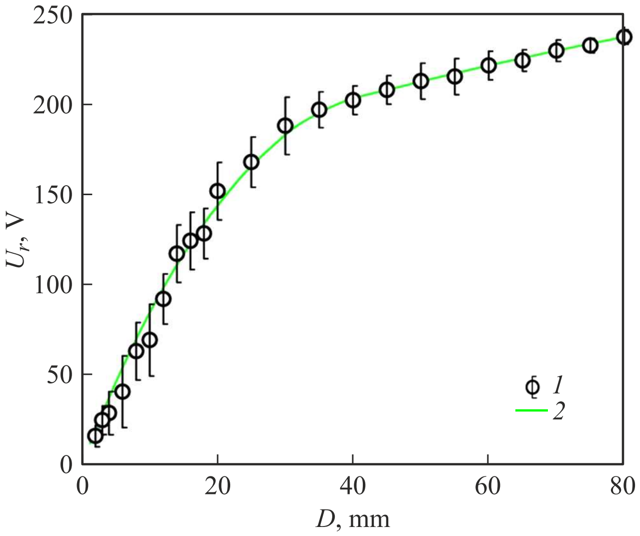

Figure 2. Size effect for the residual surface potential under electrization of PTFE films to 400 V. *1* — Experiment (with a 95% CI), *2* — optimum approximation.

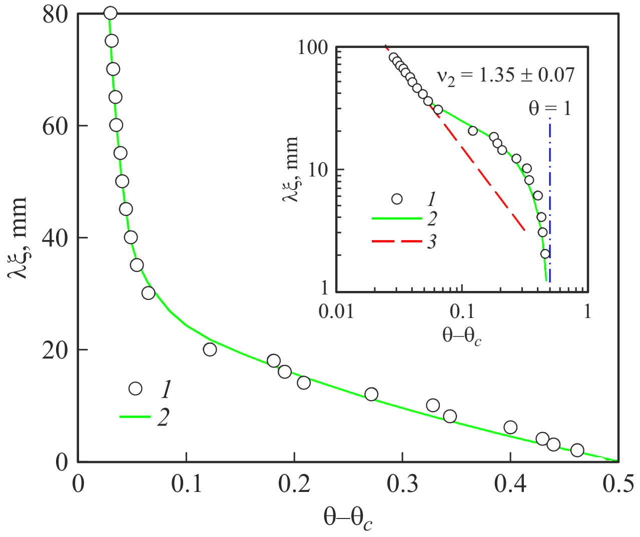

Figure 3. Dependence of the correlation length of a percolation cluster on the degree of coverage of an electrified PTFE surface by a conducting phase. The inset presents the results of determination of the critical exponent of the correlation length. The dash-and-dot line corresponds to the point of complete filling of the surface by a conducting phase ($\theta = 1$). *1* — Experiment, *2* — optimum approximation, *3* — scaling asymptote.

It is evident that, as was predicted theoretically [12], the correlation length increases as one approaches the percolation threshold. Since relation $\xi \propto |\theta - \theta_c|^{-\nu_2}$ should be satisfied in the vicinity of the percolation threshold, the slope of the scaling asymptote in a log-log scale (dashed line in the inset of Fig. 3) yields the value of critical exponent

ν_2 of the correlation length of a percolation cluster on approach to the percolation threshold. The critical exponent determined this way is $\nu_2 = 1.35 \pm 0.07$. This value agrees almost perfectly with known theoretical estimates for 2D percolation: $\nu_2 = 1.33 \pm 0.04$ [13], 1.36 ± 0.04 [14], 1.34 ± 0.02 [15], 1.35 [12], and $\nu_2 < 1.5$ [16]. A fine agreement between experimental and theoretical values of the critical exponent of the correlation length verifies the percolative nature of charge transport along an electrified surface.

Thus, the obtained experimental data indicate that the surface discharge of an electrified PTFE surface has its origins in percolation processes.

Conflict of interest

The author declares that he has no conflict of interest.

References

[1] Yu.I. Kuzmin, Tech. Phys. Lett., **25** (11), 877 (1999). DOI: 10.1134/1.1262669.

[2] K.C. Kao, *Dielectric phenomena in solids* (Elsevier Academic Press, San Diego, 2004).

[3] *Electrets*, ed. by G.M. Sessler (Springer, Berlin–Heidelberg, 1987).

[4] X. Li, Y. Wang, M. Xu, Y. Shi, H. Wang, X. Yang, H. Ying, Q. Zhang, J. Appl. Polym. Sci., **138** (19), 50406 (2021). DOI: 10.1002/app.50406

[5] P. Wei, X.L. Li, L. Wang, N.N. Liu, S. He, Y.R. Ren, Y.W. Zhu, Y.D. Yang, G.H. Lu, L.J. Bu, Adv. Electron. Mater., **6** (4), 1901156 (2020). DOI: 10.1002/aelm.201901156

[6] E.C. Plunkett, Q. Zhang, H.E. Katz, D.H. Reich, ACS Appl. Electron. Mater., **3** (4), 1656 (2021). DOI: 10.1021/acsaelm.0c01116

[7] D. Stauffer, M. Sahimi, in *Complex media and percolation theory*, ed. by M. Sahimi, A.G. Hunt. Encyclopedia of Complexity and Systems Science Ser. (Springer, N.Y., 2021), p. 49–60. DOI: 10.1007/978-1-0716-1457-0_464

[8] X. Ma, F. Zhang, X. Zhang, G. Li, P. Fang, IEEE Trans. Dielectr. Electr. Insul., **27** (5), 1439 (2020). DOI: 10.1109/TDEI.2020.008850

[9] M. Galikhanov, IEEE Trans. Dielectr. Electr. Insul., **29** (3), 788 (2022). DOI: 10.1109/TDEI.2022.3159841

[10] S.-K. Ma, *Modern theory of critical phenomena* (Taylor and Francis, N.Y., 2019). DOI: 10.4324/9780429498886

[11] P.-G. de Gennes, *Scaling concept in polymer physics* (Cornell University Press, Ithaca–London, 1979).

[12] D. Stauffer, Phys. Rep., **54** (1), 1 (1979). DOI: 10.1016/0370-1573(79)90060-7

[13] M.E. Levinshtein, B.I. Shklovskii, M.S. Shur, A.L. Efros, Sov. Phys. JETP, **42** (1), 197 (1975).

[14] A.V. Sheinman, Sov. Phys. Semicond., **9** (11), 1396 (1975).

[15] A.G. Dunn, J.W. Essam, D.S. Ritchie, J. Phys. C, **8** (24), 4219 (1975). DOI: 10.1088/0022-3719/8/24/014

[16] J. Kurkijarvi, T.C. Padmore, J. Phys. A, **8** (5), 683 (1975). DOI: 10.1088/0305-4470/8/5/005